Eur. Phys. J. A **12**, 435–446 (2001)

THE EUROPEAN PHYSICAL JOURNAL A

Chiral dynamics and the reactions pp $\longrightarrow$ d$K^+\bar{K}^0$ and pp $\longrightarrow$ d$\pi^+\eta$

E. Oset[1], J.A. Oller[2], and U.-G. Meißner[2,a]

[1] Departamento de Física Teórica and IFIC, Centro Mixto Universidad de Valencia-CSIC, Institutos de Investigación de Paterna, Aptad. 22085, 46071, Valencia, Spain
[2] Forschungszentrum Jülich, Institut für Kernphysik (Theorie), D-52425 Jülich, Germany

Received: 28 September 2001
Communicated by A. Schäfer

Abstract. We perform a study of the final-state interactions of the $K^+\bar{K}^0$ and the $\bar{K}^0 d$ systems in the reactions $pp \to dK^+\bar{K}^0$ and $pp \to d\pi^+\eta$. Since the two-meson system couples strongly to the $a_0(980)$ resonance, these reactions are expected to be an additional source of information about the controversial scalar sector. We also show that these reactions present peculiar features which can shed additional light on the much debated meson-baryon scalar sector with strangeness -1. We deduce the general structure of the amplitudes close to the $dK^+\bar{K}^0$ threshold, allowing for primary $K^+\bar{K}^0$ as well as $\pi^+\eta$ production with the two mesons in relative S- or P-wave. The interactions of the mesons are accounted for by using chiral unitary techniques, which generate dynamically the $a_0(980)$ resonance, and the $\bar{K}^0 d$ interaction is also taken into account. General formulae are derived that allow to incorporate the final-state interactions in these systems for any model of the production mechanism. We illustrate this approach by considering two specific production mechanisms based on three flavor meson-baryon chiral perturbation theory. It is demonstrated that in this scenario the $\bar{K}^0 d$ interactions are very important and can change the cross-section by as much as one order of magnitude. The amount of $\pi^+\eta$ *versus* $K^+\bar{K}^0$ production is shown to depend critically on the primary mixture of the two mechanisms, with large interference effects due to final-state interactions. These effects are also shown to occur in the event distributions of invariant masses which are drastically modified by the final-state interactions of the two-meson or the $\bar{K}d$ system.

PACS. 12.39.Fe Chiral Lagrangians – 13.75.Lb Meson-meson interactions – 13.75.Gx Kaon-baryon interactions

1 Introduction

The reaction $pp \to dK^+\bar{K}^0$ is presently the subject of experimental study by the ANKE collaboration at the Cooler Synchrotron COSY at Jülich with the aim (among others) of learning about the nature and properties of the $a_0(980)$ resonance [1]. The problem has attracted also the interest of theoretical groups [2,3](see furthermore the contributed papers in [4]). The prospect of gaining novel information about the $a_0(980)$ resonance, which might help to shed further light from the experimental side on the disputed nature of this resonance, is one of the attractive features of this reaction. This controversy originates from the observation that there are several different models to deal with the isospin $I = 0$, 1 scalar sector, all of them reproducing the scattering data to some extent, but with different conclusions with respect to the origin of the underlying dynamics. In particular, in refs. [5–9] these resonances are considered as preexisting ones (genuine quark model states), while in ref. [10] they appear as meson-meson resonances generated by a potential. In ref. [11] the advocated solution is that the $a_0(980)$ and the $f_0(980)$, the latter in the channel with $I = 0$, are exotic resonances, that is, not simply $q\bar{q}$ states, while the preexisting $q\bar{q}$ scalar nonet should be heavier, around 1.4 GeV or so. Other interesting approaches to this problem are refs. [12–16], the relativistic quark model with an instanton-induced interaction of the Bonn group [17], the Jülich meson-exchange approach [18], the Inverse Amplitude Method [19] or some variants of it [20]. It is notorious that opposite conclusions are obtained in refs. [21,22] from the use of QCD sum rules. Regarding this controversy about the nature of the scalar resonances, the works of refs. [23–28] have stressed the role of chiral symmetry and unitarity to understand the dynamics associated with the lowest-lying scalar resonances (see also [13]). As a result of the latter references the lightest 0^{++} nonet is established to be of dynamical origin, *i.e.* made up of meson-meson resonances, and is formed by the $\sigma(500)$, κ, $a_0(980)$ and a strong contribution to the physical $f_0(980)$. On the other hand, the preexisting scalar nonet would be made up by an octet

[a] e-mail: u.meissner@fz-juelich.de

around 1.4 GeV and a singlet contributing to the physical $f_0(980)$ resonance. Similar conclusions about the nature of the scalar resonances have been obtained in ref. [21] for the channels with isospin 0 and 1 within QCD sum rules. The previous set of works [23–28] constitute a unique theoretical approach to the scalar sector capable to study all these reactions in a unified way. This is achieved because all these processes are related by the use of an effective theory description that combines chiral perturbation theory and unitarity constraints.

It is important to remark, as already pointed out in ref. [12], that it is mandatory to study not only the experimental data concerning phase shifts and inelasticities related to meson-meson scattering but also production reactions where the interactions between the mesons manifest themselves through the final-state interactions (FSI). This was indeed the subject of refs. [25–28] and plays a key role in the present investigation.

In the baryon sector the studies of [29–31] based on the use of chiral Lagrangians also show that the $\Lambda(1405)$ resonance is generated in a similar way. The fact that the $\Lambda(1405)$ is of dynamical origin was pointed out already many years ago [32]. More recently it has also been shown [33] that the $\Lambda(1670)$ and the $\Sigma(1620)$ are generated dynamically in the same chiral scheme of [30]. Still, in this sector more work is needed to firmly establish these results.

As we will see, the reaction $pp \to dPQ$ (where P, Q denote pseudoscalar mesons) offers novel possibilities with respect to other reactions where the $a_0(980)$ resonance is produced since it is sensitive to *both* the meson-meson and meson-baryon final-state interactions. In particular, we stress the importance of the $\bar{K}d$ FSI, which has a very pronounced influence on observable yields, invariant-mass distributions or cross-sections, mostly through the interference with the meson-meson FSI (which gives rise to the $a_0(980)$). This should provide extra information to test the implications of chiral symmetry on the nature of the low-lying resonances.

The manuscript is organized as follows. In sect. 2, we discuss the basic reaction mechanisms for the process $pp \to dPQ$, first in very general terms and then we consider a specific model based on chiral symmetry for the primary production of the meson pair. The final-state interactions are treated in sect. 3, separately for the meson-meson and the meson-baryon systems. We stress in particular the role of the antikaon-deuteron FSI. The results are presented and discussed in sect. 4 and conclusions are drawn in sect. 5. The appendix contains a detailed discussion on the general structure of the process $pp \to dPQ$.

2 Basic reaction mechanisms

2.1 General considerations

The reaction measured in [1] is:

$$pp \to dK^+\bar{K}^0 \ . \tag{1}$$

We will study it theoretically in connection with the accompanying process

$$pp \to d\pi^+\eta \ , \tag{2}$$

since the dynamics of coupled channels, which we will use here, deals with both channels simultaneously. On the other hand, the energy of the ANKE experiment is fixed to $\sqrt{s} = 2912.88$ MeV just about 45 MeV above the $dK^+\bar{K}^0$ threshold.

The reaction (1) forces the $K^+\bar{K}^0$ system to be in a $I = 1$ state which, given the proximity of the $a_0(980)$ resonance, would have its rate of production and invariant-mass distributions very much influenced by the tail of that resonance. The reaction (2), which is also planned to be measured by the ANKE collaboration, could see the actual shape of the $a_0(980)$ resonance through the mass distribution of the $\pi^+\eta$ system.

The P-wave nature of the reaction [2,3] is another peculiar feature that makes it different to other ones producing the $a_0(980)$ [34,35]. Indeed, due to total angular momentum and parity conservation as well as to the antisymmetry of the initial state, the two mesons cannot be simultaneously in intrinsic S-wave and in S-wave relative to the deuteron. Henceforth, we denote by ℓ the orbital angular momentum of the CM motion of the two pseudoscalars PQ and the deuteron, and by L the orbital angular momentum of the pseudoscalar mesons in their own CM frame, what we also call intrinsic angular momentum of the two mesons. With this notation the cases $\ell = 1$, $L = 0$ and $\ell = 0$, $L = 1$ are possible and then the initial state is forced to have $\ell_0 = 1,\ 3$ and $S = 1$, with ℓ_0 denoting the orbital angular momentum of the initial pp state. These are the dominant contributions since they imply the lowest power, namely 1, of the small three-momenta of the deuteron or kaons in the transition amplitudes. Of course, the threshold of the reaction (2) is much lower than the one of (1) but due to the resonant nature of the interactions between the pseudoscalars, which only occurs when both $\pi^+\eta$ and $K^+\bar{K}^0$ are coupled together [23,24, 19], we will consider the same structures as well for (2). Even more, since the $\pi^+\eta$ system is expected to couple only very weakly to the P-waves then only the structure with $\ell = 1$, $L = 0$ is kept for $\pi^+\eta$. The fact that either $\ell = 1$ or $L = 1$ has its relevance since, close to threshold, one would expect to have all particles in a S-wave. Thus, the $K^+\bar{K}^0$ system would be in an intrinsic S-wave state subject to the full strength of the $a_0(980)$ resonance tail. However, in the present case the contributions with $L = 0$ or 1 are of the same order of magnitude. Furthermore, as commented above, if the $\pi^+\eta$ system does couple just weakly to the P-waves, as we will argue below that this is the expected behaviour, then the reaction mechanism establishes a distinction between the $K^+\bar{K}^0$ and $\pi^+\eta$ production processes which is novel with respect to other threshold production reactions.

The reaction mechanisms for $K^+\bar{K}^0$ and $\pi^+\eta$ production are complicated. Some approximate models have been used in refs. [2,3] based on direct production of the $a_0(980)$ resonance. The $\pi^+\eta$ production channels are not studied

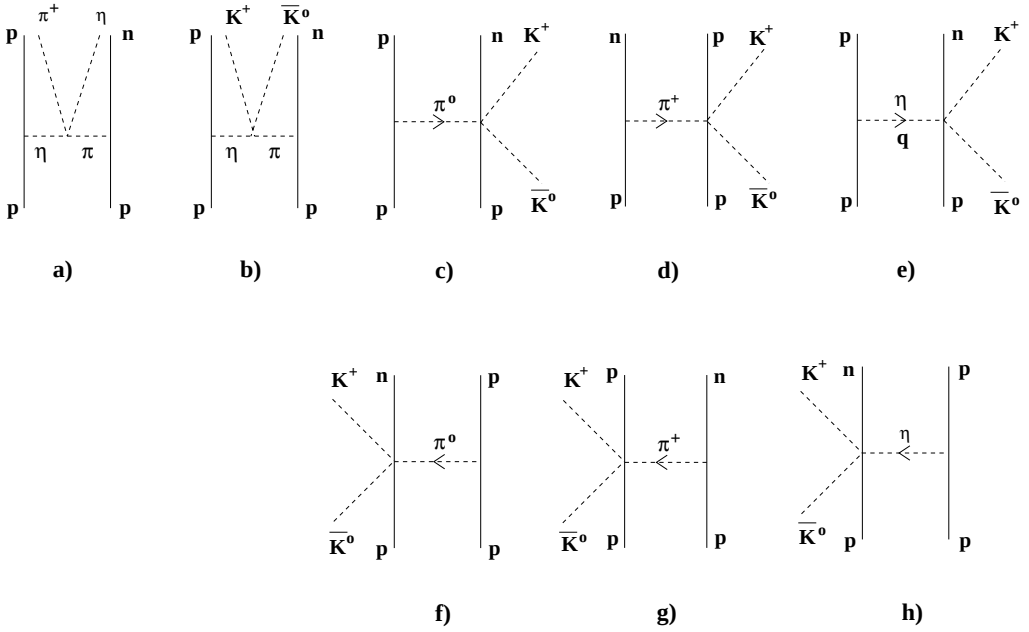

Fig. 1. Chiral model for the primary production used to extract the structures given in eq. (7).

there although they could in principle be accounted for by using partial decay rates of the $a_0(980)$ into $K\bar{K}$ and $\pi\eta$ [36]. However, the arguments given above about the unique prospects of this reaction indicate that the rates could be quite different in the present process than those determined by making use of standard Breit-Wigner parameterizations or related ones. Thus, substantial deviations from the rates observed in the present reaction would give further support to the method of coupled-channel generation of that resonance as the appropriate tool to deal with the light scalar resonances, *versus* static pictures that consider this resonance as an object with predetermined decay rates into different channels, and the final-state interactions are just taken into account via Breit-Wigner-like modifications of the resonance propagator. Indeed, inconsistencies in the treatment of the related $f_0(980)$ resonance as a pure Breit-Wigner or following a Flatté formula have been recently pointed out in ref. [37] in the reaction $\phi \to \gamma\pi^0\pi^0$.

2.2 Dynamical model based on chiral symmetry

Since we are interested in stressing the role of the final-state interactions of the $K\bar{K}$ and $\bar{K}d$ systems we refrain from searching for a complete model and simply parameterize the original structure of the amplitude close to the $dK\bar{K}$ threshold, the region of interest for the ANKE collaboration. This is done in appendix A. Nevertheless, the number of free parameters when allowing for the general structure deduced in appendix A is too large to draw any definite conclusion. To overcome this difficulty we consider in the following a specific model derived from lowest-order three-flavor chiral perturbation theory (CHPT) [38–40] depicted in fig. 1, giving rise to two definite structures which already illustrate the main points of our investigation, namely, the extreme importance of the final-state interactions between the mesons and between the $\bar{K}^0$ and the deuteron. Then a variety of observables are evaluated in terms of the two parameters of the theory, up to a global normalization which will not be needed to evaluate ratios of cross-sections and invariant-mass distributions nor to compare with the future ANKE results. It is worth stressing that, given any model accounting for the primary production of the $dK^+\bar{K}^0$ and $d\pi^+\eta$ systems, the final-state interactions can be taken into account following the general scheme presented in appendix A.

Let us come back to fig. 1. Such diagrams involving the production of two mesons were evaluated in ref. [41] and have a similar structure, with some cancellations among them. In order to see this structure we consider diagrams 1c) and 1e). The two-baryon-three-meson (BBMMM) vertices are given by [41]

$$\mathcal{L}_1^{(B)} = \frac{1}{2}(D+F)\left(\bar{n}\gamma^\mu\gamma_5 u_\mu^{(21)} p + \bar{p}\gamma^\mu\gamma_5 u_\mu^{(11)} p\right) \ , \quad (3)$$

where u_μ is a $SU(3)$ matrix containing the meson fields which is given explicitly in [41]. Furthermore, $D \simeq 3/4$ and $F \simeq 1/2$ are the canonical $SU(3)$ axial coupling constants. The relevant terms for our case are contained in the $u_\mu^{(21)}$ and $u_\mu^{(11)}$ matrix elements, and keeping in mind the non-relativistic reduction of $\gamma^\mu\gamma_5$, are proportional to:

$$u_\mu^{(21)} \to \frac{3}{\sqrt{2}}\pi^0\left(\partial_\mu K^0 K^- - \partial_\mu K^- K^0\right) + \sqrt{6}\,\partial_\mu\eta K^0 K^- \ ,$$
$$u_\mu^{(11)} \to \partial_\mu\pi^+ K^0 K^- + \pi^+\partial_\mu K^- K^0 - 2\pi^+\partial_\mu K^0 K^- \ . \quad (4)$$

Thus, diagram 1c), with a non-relativistic reduction of $\gamma^\mu\gamma_5$ leads to a structure

$$\frac{3}{\sqrt{2}}\boldsymbol{\sigma}^{(2)}(\mathbf{p}_{K^+}-\mathbf{p}_{\bar{K}^0})\ , \tag{5}$$

which produces the $K\bar{K}$ system with a relative P-wave, while diagram 1e) leads to a structure

$$\sqrt{6}\boldsymbol{\sigma}^{(2)}\mathbf{q}\ , \tag{6}$$

where the superscript 1(2) applies to the the baryon line to the left(right) side of fig. 1. In addition, the initial proton on the left(right) baryon line has three-momenta $\mathbf{p}_1(\mathbf{p}_2)$.

The global structure of the amplitude is obtained by considering also the $\boldsymbol{\sigma}^{(1)}\mathbf{q}$ vertex in the meson baryon vertex to the left side of the diagram. By taking $\mathbf{q} = \mathbf{p}_1 - \mathbf{p}_d/2$, with $\mathbf{p}_1$, $\mathbf{p}_d$ the momenta of the initial proton and the deuteron, respectively (we have checked that consideration of the Fermi motion in the deuteron does not change the final structure), we find two types of terms:

$$\begin{aligned}
&\text{I)}\ \ \boldsymbol{\sigma}^{(1)}(\mathbf{p}_1-\mathbf{p}_d/2)\,\boldsymbol{\sigma}^{(2)}(\mathbf{p}_{K^+}-\mathbf{p}_{\bar{K}^0})\\
&\quad -\boldsymbol{\sigma}^{(1)}(\mathbf{p}_{K^+}-\mathbf{p}_{\bar{K}^0})\,\boldsymbol{\sigma}^{(2)}(\mathbf{p}_2-\mathbf{p}_d/2)\ ,\\
&\text{II)}\ \boldsymbol{\sigma}^{(1)}(\mathbf{p}_1-\mathbf{p}_d/2)\,\boldsymbol{\sigma}^{(2)}(\mathbf{p}_1-\mathbf{p}_d/2)\\
&\quad -\boldsymbol{\sigma}^{(1)}(\mathbf{p}_2-\mathbf{p}_d/2)\,\boldsymbol{\sigma}^{(2)}(\mathbf{p}_2-\mathbf{p}_d/2)\ ,
\end{aligned} \tag{7}$$

which would come from the sum of the diagrams 1c) and f), for eq. (7.I), and diagrams 1e) and h), for eq. (7.II), after taking into account the isospin zero of the deuteron. Also the deuteron wave function appears with its value at the origin, $\phi(0)$, in coordinate space neglecting the range of the interaction, since the propagators of the pseudoscalar mesons in fig. 1 carry very high momentum transfers. In order to take into account the antisymmetry of the initial pp state we must subtract to the previous expressions the same amplitudes exchanging the two initial protons. This means both spin and momentum but, since we have $S = 1$ in the initial state, the wave function is spin symmetric and then it is enough to subtract the amplitudes of eq. (7) exchanging $\mathbf{p}_1 \leftrightarrow \mathbf{p}_2 = -\mathbf{p}_1$. This leads, up to a global factor two, to the structures:

$$\begin{aligned}
&\text{I)}\ \ \boldsymbol{\sigma}^{(1)}\mathbf{p}_1\,\boldsymbol{\sigma}^{(2)}(\mathbf{p}_{K^+}-\mathbf{p}_{\bar{K}^0})+\boldsymbol{\sigma}^{(1)}(\mathbf{p}_{K^+}-\mathbf{p}_{\bar{K}^0})\,\boldsymbol{\sigma}^{(2)}\mathbf{p}_1\ ,\\
&\text{II)}\ -\boldsymbol{\sigma}^{(1)}\mathbf{p}_1\,\boldsymbol{\sigma}^{(2)}\mathbf{p}_d-\boldsymbol{\sigma}^{(1)}\mathbf{p}_d\,\boldsymbol{\sigma}^{(2)}\mathbf{p}_1\ .
\end{aligned} \tag{8}$$

This calculation would not be complete to account for the π exchange because the explicit use of the isospin deuteron wave function forces also the simultaneous consideration of diagrams 1d) and g) with the exchange of a charged pion. The structure of these two latter diagrams is different than the structure of eq. (7.I) found for π^0 exchange, but it is easy to see that it is a combination of eqs. (7.I), (7.II) and after antisymmetrization with respect to the initial state leads again to the structures of eqs. (8).

Should the $K\bar{K}$ system be in an intrinsic S-wave, $L = 0$, we would have eq. (8.II) and the cross-section contains the factor $\mathbf{p}_d^{\,2}$, as correctly stated in ref. [42], which largely affects the shape of the $K\bar{K}$ invariant-mass distribution.

As already mentioned, we will also consider $\pi^+\eta$ production. One interesting property of the $\pi\eta$ system reflected in chiral dynamics is that it does not couple in P-waves to lowest order in the chiral counting [43]. It does not couple to vector mesons either [44]. It can couple in higher orders but such effects are suppressed by more than one order of magnitude with respect to the dominant S-waves [43]. This means that there are no terms of the type of diagram 1c), d) or e) with the structure of eq. (5), and in fact what one finds is that the matrix elements $u_\mu^{(21)}$ and $u_\mu^{(11)}$ of eq. (3) do not contain any $\pi\pi\eta$ or $\eta\eta\pi$ terms. However, terms of the type of diagram 1a), with the $\pi\eta$ system in S-wave are allowed leading to a structure of the global amplitude of type II in eq. (8). The same comment applies to fig. 1b) with respect to the $K^+\bar{K}^0$ state.

One still has to take into account that in the experiment only unpolarized observables are measured. This implies an equal probability for the initial state of being in any of the three possible total-spin projections. Taking the vector $\mathbf{Q}$ to represent either $\mathbf{p}_{K^+} - \mathbf{p}_{\bar{K}^0}$ or $\mathbf{p}_d$, any of the structures shown in eq. (8) can be written as $\mathcal{A} \equiv \boldsymbol{\sigma}^{(1)}\mathbf{p}_1\,\boldsymbol{\sigma}^{(2)}\mathbf{Q} + \boldsymbol{\sigma}^{(1)}\mathbf{Q}\,\boldsymbol{\sigma}^{(2)}\mathbf{p}_1$. It is straightforward to see that the matrix elements between states $|S\,S_3\rangle$ of well defined third component S_3 and total-spin $S = 1$ satisfy

$$\langle 1\beta|\mathcal{A}|1\alpha\rangle = \eta_{\alpha\beta}\frac{4\sqrt{\pi}}{\sqrt{3}}\,|\mathbf{p}_1||\mathbf{Q}|\,\mathrm{Y}_{1\,\alpha-\beta}(\hat{Q})\ , \tag{9}$$

with $\hat{Q}$ the unit vector in the direction of $\mathbf{Q}$, $\mathrm{Y}_{Lm}(\theta,\phi)$ the usual spherical harmonics and the matrix $\eta_{\alpha\beta}$ is given by:

$$\eta = \begin{pmatrix} +1 & -1 & 0 \\ +1 & -1 & +1 \\ 0 & -1 & +1 \end{pmatrix}\ . \tag{10}$$

In this matrix the rows correspond to $\alpha = +1,\ 0,\ -1$, in order, and analogously for the columns. We have also taken $\mathbf{p}_1$ parallel to the z-axis, that is, $\mathbf{p}_1 = (0, 0, |\mathbf{p}_1|)$.

The structures and couplings of the amplitudes discussed here could be evaluated in explicit microscopic models. Given the large energies involved, there could be many competing mechanisms some of which would require information, like partial decays of resonances, which is not available at present. Given these limitations our choice provides a reasonable and simple starting point from the phenomenological side. It also illustrates the use of appendix A in order to take care of the final-state interactions in any other model.

3 Final-state interactions

In this section we first discuss the FSI due to the meson-meson interactions and then we will also consider the FSI from the $\bar{K}d$ channel. Afterwards, we sum up both contributions giving rise to our final renormalized amplitudes.

3.1 Meson-meson final-state interactions

The $K^+\bar{K}^0$ system in $I = 1$ will interact strongly and couple to the $\pi^+\eta$ system. In [23] the input of the lowest-order chiral Lagrangian was used as the kernel (potential) of the Bethe-Salpeter equation which produced exact unitarization in coupled channels. The extension in [19,24] to include effects from higher-order Lagrangians, crossed channel dynamics, explicit exchange of genuine resonance states and scale independence did not modify the properties of the scalar sector found in [23] with only the lowest-order Lagrangian and a cut-off of natural size, about 1 GeV, to regularize the loops. Since the divergences were only logarithmic, the numerics are not changed when this cut-off is substituted by a regularization scale $\mu \sim 1$ GeV and a subtraction constant that can be calculated in terms of the cut-off, see, *e.g.* [45,31,33] [1]. Hence, given the simplicity and accuracy of ref. [23], which is a limiting case of the more general formalism developed in [24] (see, *e.g.* [46, 47]), we will use this approach in our present problem.

Diagrammatically it means that in addition to the tree-level diagrams of fig. 1 we will have the diagrams of fig. 2 which contribute to the $K^+\bar{K}^0$ production in the first line and to $\pi^+\eta$ production in the second one. By calling G the loop function of the mesons, the sums in fig. 2 will dress the structure, eq. (8.II), containing the $\mathbf{p}_d$ vector corresponding to the case when the two mesons are in S-wave in their CM reference system, $L = 0$. So we will have:

$$\pi^+\eta : f^S_{\pi\eta}|\mathbf{p}_1||\mathbf{p}_d|\mathrm{Y}_{1m}(\hat{p}_d) \to |\mathbf{p}_1||\mathbf{p}_d|\mathrm{Y}_{1m}(\hat{p}_d) \times\left(f^S_{\pi\eta} + f^S_{\pi\eta}G_{\pi\eta}t_{\pi\eta\to\pi\eta} + f^S_{K\bar{K}}G_{K\bar{K}}t_{K\bar{K}\to\pi\eta}\right) ,$$

$$K^+\bar{K}^0 : f^S_{K\bar{K}}|\mathbf{p}_1||\mathbf{p}_d|\mathrm{Y}_{1m}(\hat{p}_d) \to |\mathbf{p}_1||\mathbf{p}_d|\mathrm{Y}_{1m}(\hat{p}_d) \times\left(f^S_{K\bar{K}} + f^S_{K\bar{K}}G_{K\bar{K}}t_{K\bar{K}\to K\bar{K}} + f^S_{\pi\eta}G_{\pi\eta}t_{\pi\eta\to K\bar{K}}\right), \quad (11)$$

where the subscript m corresponds to $\alpha-\beta$ in the notation of eq. (9), all the three-momenta refer to the CM frame of the pp system and f^S_{PQ} are the couplings of the two pseudoscalar meson systems with $L = 0$. The latter are defined such that the minus global sign in eq. (8.II) is reabsorbed by them. Equations (11) are more elegantly written in a 2×2 matrix form as:

$$|\mathbf{p}_1||\mathbf{p}_d|\mathrm{Y}_{1m}(\hat{p}_d)\,(1 + t\,G)\left\{\begin{array}{c} f^S_{\pi\eta} \\ f^S_{K\bar{K}}\end{array}\right\} , \quad (12)$$

with t_{ij} the S-wave transition matrix $K\bar{K},\ \pi\eta \to K\bar{K},\ \pi\eta$ in $I = 1$ with index "1" for $\pi\eta$ and index "2" for $K\bar{K}$, and G a diagonal matrix $G = \mathrm{diag}(G_{\pi\eta}, G_{K\bar{K}})$. Now taking into account the Bethe-Salpeter equation and the on-shell factorization of the potential in the loop functions involved in the strong interactions proved in [23]:

$$t = t_2 + t_2 \cdot G \cdot t\ ; \quad t = [1 - t_2 \cdot G]^{-1}\cdot t_2\ , \quad (13)$$

[1] While the explicit calculations have been done in dimensional regularization, this statement holds for any mass-independent regularization scheme.

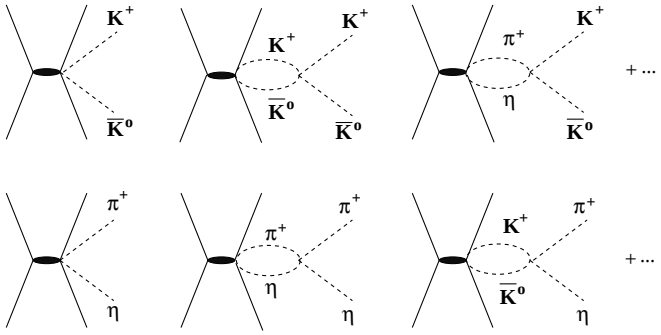

Fig. 2. Diagrams relevant to take into account the meson-meson FSI. The $a_0(980)$ resonance is dynamically generated through the iteration of the meson-meson bubbles. This iteration is indicated in the figure by the ellipses.

where t_2 contains the corresponding lowest-order CHPT meson-meson scattering amplitudes [23], we can write eq. (12) as:

$$|\mathbf{p}_1||\mathbf{p}_d|\mathrm{Y}_{1m}(\hat{p}_d)\,\mathcal{D}^{-1}\left\{\begin{array}{c} f^S_{\pi\eta} \\ f^S_{K\bar{K}}\end{array}\right\} , \quad (14)$$

where $\mathcal{D} = [1 - t_2 \cdot G]$. Both t and G are functions of the invariant mass of the meson-meson system, M_I^2. The previous formalism to take into account FSI was originally employed in the calculation of $\gamma\gamma$ →meson-meson in ref. [25] and later systematized in more general terms taking into account the analytic properties of the form factors in refs. [28,48]. In these last references it can be seen that the above results for taking care of the FSI are exact when considering only the right hand or unitarity cut. We will take the functions $f^S_{\pi\eta}$ and $f^S_{K\bar{K}}$ as constants since we are concerned in the energy region available to the ANKE collaboration which reduces to just about 45 MeV above the $K^+\bar{K}^0$ threshold. Our approach of taking care only of the right-hand cut corresponds to the expected dominance of the resonances $a_0(980)$ and $\Lambda(1405)$ which are very close to the $dK^+\bar{K}^0$ threshold. The chiral model of subsect. 2.2 gives rise to real couplings $f^S_{\pi\eta}$ and $f^S_{K\bar{K}}$, and so we will take them in the following. Nevertheless, the results of appendix A can be equally applied to real or complex coupling functions $f^S_{\pi\eta}$ and $f^S_{K\bar{K}}$.

3.2 Antikaon-deuteron final-state interactions

Now we consider the FSI from the $\bar{K}d$ system. The interaction of the K^+ with the protons and neutrons is rather weak [29] and we will neglect it. However, this is not the case for the $\bar{K}^0n$ interactions which are very strong close to threshold due to the $\Lambda(1405)$ resonance below the $\bar{K}^0n$ threshold [32,29–31]. On the other hand, what we need here is the $\bar{K}^0$ interaction with the deuteron that is quite strong close to the threshold due to extra reinforcement of the multiple scattering of the $\bar{K}$ in the deuteron as proved in multiple evaluations of this quantity using Faddeev equations [49–53]. A reanalysis of this quantity to the light of the new $\bar{K}N$ amplitudes generated in the chiral dynamical approach of [30] was done in [54] within

the fixed scatterer approximation for the deuteron, which proves rather accurate comparing the results with those of the non-static calculation of [53]. A sizeable $\bar{K}d$ scattering length of about $(-1.6+i1.9)$ fm is obtained in [54]. In order to take into account this extra interaction, we first extrapolate the results of the $\bar{K}d$ scattering amplitude at threshold of [54] to the small finite $\bar{K}$ energies of the ANKE experiment [1]. For this purpose, we rely upon the results for the $\bar{K}N$ scattering matrix found in [30](fig. 9) which show a drastic reduction of the real part of $t_{K^-p} + t_{K^-n}$ at $\sqrt{s} \simeq 1450$ MeV. Taking into account this fact plus the approximate good results of the impulse approximation for the imaginary part of the $\bar{K}d$ scattering length and the fast decline of the real part of the amplitudes from threshold on, suggest a quadratic interpolation between the results at threshold and the impulse approximation at $\sqrt{s} \simeq 1450$ MeV and beyond. Hence, for the general and illustrative purposes of the present chiral model to the primary production amplitudes of the $K\bar{K}$ and $\pi\eta$ channels, the following parameterization is expected to provide a sufficiently accurate description of the $\bar{K}d$ scattering amplitude:

$$\mathrm{Re}\; t_{\bar{K}d}(\widetilde{M}_B) = a(\widetilde{M}_B - \widetilde{M}_{B0})^2 + b(\widetilde{M}_B - \widetilde{M}_{B_0}) + c\;, \quad (15)$$

with

$$a = 4.32 \cdot 10^{-4}\,\mathrm{MeV}^{-3}\;, \quad b = -1.55 \cdot 10^{-2}\,\mathrm{MeV}^{-2}\;,$$
$$c = 0.13\,\mathrm{MeV}^{-1}\;, \qquad \widetilde{M}_{B_0} = 1432\,\mathrm{MeV}\;, \quad (16)$$

where $\widetilde{M}_B^2 = (p_{\bar{K}^0} - p_d/2)^2$ is the invariant mass of the $\bar{K}^0$ and the neutron in the deuteron. The imaginary parts are well approximated by the impulse approximation and are almost constants in the whole interval. We take finally

$$\mathrm{Im}\; t_{\bar{K}d}(\widetilde{M}_B) = b'(\widetilde{M}_B - \widetilde{M}_{B_0}) + c'\,, \quad (17)$$

with

$$b' = 1.1 \cdot 10^{-3}\,\mathrm{MeV}^{-2}\;, \quad c' = -1.5 \cdot 10^{-1}\,\mathrm{MeV}^{-1}\;. \quad (18)$$

We apply the formulae (15) and (17) for $\widetilde{M}_B < 1.45$ GeV, and

$$t_{\bar{K}d}(\widetilde{M}_B) = t_{\bar{K}d}(1.45\ \mathrm{GeV})\;, \quad (19)$$

for $\widetilde{M}_B > 1.45$ GeV. We have also checked that substituting this limiting value by a larger one only modifies mildly the resulting distributions.

The implementation of the FSI of $\bar{K}d$ requires to rewrite the amplitudes of eq. (9), for $\mathbf{Q} = \mathbf{p}_{K^+} - \mathbf{p}_{\bar{K}^0}$ and $\mathbf{Q} = \mathbf{p}_d$ in the rest frame of the $\bar{K}d$. This is easily done by taking into account momentum conservation and the fact that $\mathbf{p}_{K^+} - \mathbf{p}_{\bar{K}^0}$ is a Galilean invariant. Given the small velocities involved in the $dK^+\bar{K}^0$ system, we find it appropriate to just apply Galilean transformations. Let us first consider the intrinsic P-wave meson-meson contribution, eq. (8.I). In the following we denote by $\mathbf{p}_\ominus = \mathbf{p}_{K^+} - \mathbf{p}_{\bar{K}^0}$, and hence this contribution involves $\mathrm{Y}_{1m}(\hat{p}_\ominus)$. Since we are considering Galilean invariance $\mathbf{p}_\ominus = \mathbf{p}\,'_\ominus$, we then can rewrite $|\mathbf{p}_\ominus|\mathrm{Y}_{1m}(\hat{p}_\ominus)$ as:

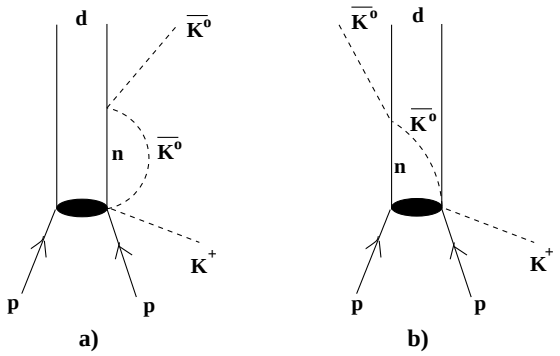

Fig. 3. Diagrams to take into account the $\bar{K}^0 d$ FSI.

$$|\mathbf{p}_\ominus|\mathrm{Y}_{1m}(\hat{p}_\ominus) = |\mathbf{p}_\ominus|\mathrm{Y}_{1m}(\hat{p}\,'_\ominus) = |\mathbf{p}\,'_{K^+}|\mathrm{Y}_{1m}(\hat{p}\,'_{K^+}) - |\mathbf{p}\,'_{\bar{K}^0}|\mathrm{Y}_{1m}(\hat{p}\,'_{\bar{K}^0}), \quad (20)$$

where the primes stand for variables in the $\bar{K}^0 d$ rest frame. The term $\mathrm{Y}_{1m}(\hat{p}\,'_{\bar{K}^0})$ involves the P-wave contribution of the $\bar{K}^0$ and hence we neglect its modification in the present case of low $\bar{K}^0$ energies. The term $\mathrm{Y}_{1m}(\hat{p}\,'_{K^+})$ does not depend on $\mathbf{p}\,'_{\bar{K}^0}$. This implies that the deuteron and $\bar{K}^0$ are in a relative S-wave and can suffer the strong $\bar{K}d$ interaction. The $\bar{K}d$ FSI are diagrammatically represented in fig. 3. and the corresponding terms are renormalized by changing them by

$$1 + \mathrm{G}_d\, t_{\bar{K}d}\;, \quad (21)$$

where G_d is the meson-deuteron loop function for the $\bar{K}N$ interaction. However, although the deuteron effects appear only as recoil corrections with respect to the nucleon meson-baryon G_N loop function these effects can be around $m_K/M_d \simeq 25\%$ due to the large mass of the kaon, cf. fig. 3b). The function G_N is given in [31] using dispersion relations and a subtraction constant $a_{\bar{K}N} = -1.82$ as needed in the approach of [33] to reproduce the low-energy $\bar{K}N$ results of [30] using a cut-off to regularize the loops. Because of the already-mentioned recoil effects and the large momentum transfer (through the shaded areas in fig. 3), we identify $\mathrm{G}_d = G_N$ but allow for a variation of $\sim 30\%$ in $a_{\bar{K}N}$. Therefore, we present results for $a_{\bar{K}N} = -1.84$ and -1.3. Having said this, we find that eq. (20) is renormalized by the FSI as:

$$|\mathbf{p}\,'_{K^+}|\mathrm{Y}_{1m}(\hat{p}\,'_{K^+})\,(1 + \mathrm{G}_d\, t_{\bar{K}d}) - |\mathbf{p}\,'_{\bar{K}^0}|\mathrm{Y}_{1m}(\hat{p}\,'_{\bar{K}^0})\;. \quad (22)$$

Now, taking into account the following equalities:

$$\mathbf{p}\,'_{K^+} = \mathbf{p}_{K^+}\frac{M_d + 2m_K}{M_d + m_K}\;,$$
$$\mathbf{p}\,'_{\bar{K}^0} = \mathbf{p}_{\bar{K}^0} + \mathbf{p}_{K^+}\frac{m_K}{M_d + m_K}\;, \quad (23)$$

it is then straightforward to rewrite eq. (22) as:

$$f^P_{K\bar{K}}|\mathbf{p}_1| \left[|\mathbf{p}_{K^+}|\mathrm{Y}_{1m}(\hat{p}_{K^+})\left(2 + \frac{M_d + 2m_K}{M_d + m_K}\mathrm{G}_d\, t_{\bar{K}d}\right) + |\mathbf{p}_d|\mathrm{Y}_{1m}(\hat{p}_d)\right]\;, \quad (24)$$

where we have multiplied the previous structure by the $K^+\bar{K}^0$ P-wave coupling $f^P_{K\bar{K}}$ times $|\mathbf{p}_1|$, since both factors appear in the original production process. In addition, $M_d = 1875.61$ MeV is the deuteron mass and $m_K = 495.7$ MeV $= (m_{K^+} + m_{\bar{K}^0})/2$, with $m_{K^+} = 493.677$ MeV and $m_{\bar{K}^0} = 497.672$ MeV the K^+ and K^0 masses, respectively.

We can follow similar steps to take into account the FSI of the $\bar{K}^0 d$ to the CM meson-meson S-wave contribution, $L = 0$, eq. (8.II). Considering the identity

$$\mathbf{p}_d = -\mathbf{p}\,'_{K^+}\frac{M_d}{M_d + 2m_K} - \mathbf{p}\,'_{\bar{K}^0}\ , \tag{25}$$

it then follows:

$$|\mathbf{p}_d|\mathrm{Y}_{1m}(\hat{p}_d) = -|\mathbf{p}_{K^+}|\mathrm{Y}_{1m}(\hat{p}\,'_{K^+})\frac{M_d}{M_d+m_K} - |\mathbf{p}\,'_{\bar{K}^0}|\mathrm{Y}_{1m}(\hat{p}\,'_{\bar{K}^0})\ . \tag{26}$$

As discussed above the $\mathrm{Y}_{1m}(\hat{p}\,'_{\bar{K}^0})$ term involves pure P-wave and it is not renormalized by the strong $\bar{K}^0 d$ interaction. Its full contribution is then accounted for by eq. (14). Hence only the term proportional to $\mathrm{Y}_{1m}(\hat{p}\,'_{K^+}) = \mathrm{Y}_{1m}(\hat{p}_{K^+})$, eq. (23), is renormalized due to the S-wave $\bar{K}^0 d$ interaction as

$$-f^S_{K\bar{K}}|\mathbf{p}_1||\mathbf{p}_{K^+}|\mathrm{Y}_{1m}(\hat{p}_{K^+})\frac{M_d}{M_d+m_K}\mathrm{G}_d\, t_{\bar{K}d}\ , \tag{27}$$

multiplied by the corresponding coupling constant $f^S_{K\bar{K}}$ already introduced in eq. (11).

3.3 Renormalized amplitudes

Once we have taken into account the important FSI due to the resonant meson-meson and $\bar{K}^0 d$ interactions, eqs. (14), (24) and (27), the renormalized $d\pi^+\eta$, $F_{\pi^+\eta}$, and $dK^+\bar{K}^0$, $F_{K^+\bar{K}^0}$, production amplitudes, corresponding to the transition between total-spin third components $\alpha \to \beta$, read

$$\frac{\sqrt{3}}{4\sqrt{\pi}}F_{\pi^+\eta} = \eta_{\alpha\beta}|\mathbf{p}_1||\mathbf{p}_d|\mathrm{Y}_{1\,\alpha-\beta}(\hat{p}_d)\Big[[\mathcal{D}^{-1}(M_I^2)]_{11}f^S_{\pi\eta} + [\mathcal{D}^{-1}(M_I^2)]_{12}f^S_{K\bar{K}}\Big]\ ,$$

$$\begin{aligned}\frac{\sqrt{3}}{4\sqrt{\pi}}\ F_{K^+\bar{K}^0} &= \eta_{\alpha\beta}|\mathbf{p}_1||\mathbf{p}_d|\mathrm{Y}_{1\,\alpha-\beta}(\hat{p}_d)\Big[[\mathcal{D}^{-1}(M_I^2)]_{21}f^S_{\pi\eta} + [\mathcal{D}^{-1}(M_I^2)]_{22}f^S_{K\bar{K}} + f^P_{K\bar{K}}\Big]\\ &+\eta_{\alpha\beta}|\mathbf{p}_1||\mathbf{p}_{K^+}|\mathrm{Y}_{1\,\alpha-\beta}(\hat{p}_{K^+})\\ &\times\left[\frac{-M_d}{M_d+m_K}f^S_{K\bar{K}}\mathrm{G}_d(\widetilde{M}_B^2)\,t_{\bar{K}d}(\widetilde{M}_B) + f^P_{K\bar{K}}\left(2+\frac{M_d+2m_K}{M_d+m_K}\mathrm{G}_d(\widetilde{M}_B^2)\,t_{\bar{K}d}(\widetilde{M}_B)\right)\right].\end{aligned} \tag{28}$$

The double invariant-mass distributions are obtained straightforwardly from the previous equations after summing over the final-state polarizations and averaging over the initial ones. In this way one has

$$\begin{aligned}\frac{\mathrm{d}^2\sigma_{\pi^+\eta}}{\mathrm{d}M_I\mathrm{d}M_B} =& 16\pi\mathcal{C}\frac{|\mathbf{p}_1|}{s^{3/2}}\theta(1-|\cos\theta_{\pi^+}|)M_I M_B|\mathbf{p}_d|^2\\ &\times\left|[\mathcal{D}^{-1}(M_I^2)]_{11}f^S_{\pi\eta} + [\mathcal{D}^{-1}(M_I^2)]_{12}f^S_{K\bar{K}}\right|^2\ ,\end{aligned}$$

$$\begin{aligned}\frac{\mathrm{d}^2\sigma_{K^+\bar{K}^0}}{\mathrm{d}M_I\mathrm{d}M_B} =& 16\pi\mathcal{C}\frac{|\mathbf{p}_1|}{s^{3/2}}\theta(1-|\cos\theta_{K^+}|)M_I M_B\Bigg\{|\mathbf{p}_d|^2\\ &\times\left|[\mathcal{D}^{-1}(M_I^2)]_{21}f^S_{\pi\eta}\right.\\ &\left.+\,[\mathcal{D}^{-1}(M_I^2)]_{22}f^S_{K\bar{K}} + f^P_{K\bar{K}}\right|^2\\ &+|p_{K^+}|^2\left|\frac{-M_d}{M_d+m_K}f^S_{K\bar{K}}\mathrm{G}_d(\widetilde{M}_B^2)\,t_{\bar{K}d}(\widetilde{M}_B)\right.\\ &\left.+f^P_{K\bar{K}}\left[2+\frac{M_d+2m_K}{M_d+m_K}\mathrm{G}_d(\widetilde{M}_B^2)\,t_{\bar{K}d}(\widetilde{M}_B)\right]\right|^2\\ &+2|\mathbf{p}_d||\mathbf{p}_{K^+}|\cos\theta_{K^+}\ \mathrm{Re}\left[\left([\mathcal{D}^{-1}(M_I^2)]_{21}f^S_{\pi\eta}\right.\right.\\ &\left.\left.+[\mathcal{D}^{-1}(M_I^2)]_{22}f^S_{K\bar{K}} + f^P_{K\bar{K}}\right)^\star\left(\frac{-M_d}{M_d+m_K}\right.\right.\\ &\left.\left.\times f^S_{K\bar{K}}\mathrm{G}_d(\widetilde{M}_B^2)\,t_{\bar{K}d}(\widetilde{M}_B) + f^P_{K\bar{K}}\right.\right.\\ &\left.\left.\times\left[2+\frac{M_d+2m_K}{M_d+m_K}\mathrm{G}_d(\widetilde{M}_B^2)t_{\bar{K}d}(\widetilde{M}_B)\right]\right)\right]\Bigg\},\end{aligned} \tag{29}$$

with $s = (p_1 + p_2)^2$ for the two protons in the initial state ($\sqrt{s} = 2912.88$ MeV for the ANKE kinematics considered here), M_B is the corresponding ηd or $\bar{K}^0 d$ invariant mass and $\mathcal{C}$ is a normalization constant. The cosine of the angle between $\mathbf{p}_{\pi^+}(\mathbf{p}_{K^+})$ and $\mathbf{p}_d$, $\cos\theta_{\pi^+}(\cos\theta_{K^+})$, can be written in terms of M_I, M_B. By integrating with respect to M_I or M_B in eq. (29) we can obtain the invariant-mass distributions with respect to M_B and M_I, respectively.

4 Results and discussion

Apart from the absolute normalization of the amplitudes, our chiral model for the primary production depends on two free parameters, θ and ϕ, such that

$$f^S_{K\bar{K}} = \cos\theta\ ,\ f^S_{\pi\eta} = \sin\theta\cos\phi\ ,\ f^P_{K\bar{K}} = \sin\theta\sin\phi\ . \tag{30}$$

First, in order to show the relevance of the FSI, we take $\theta = \phi = 0$, implying $f^S_{\pi\eta} = 0$ and $f^P_{K\bar{K}} = 0$. In fig. 4 we display several curves corresponding to $\mathrm{d}\sigma_{K^+\bar{K}^0}/\mathrm{d}M_I$ neglecting either the two considered FSI and including either one or two of them. In the rest of this section we take $a_{\bar{K}N} = -1.84$ unless the contrary is explicitly stated. The distribution in the absence of any FSI (dotted line) peaks around $M_I = 1003$ MeV. If the $K^+\bar{K}^0$ interaction is switched on (dashed line) the strength is shifted considerably towards low invariant-mass and the peak moves to

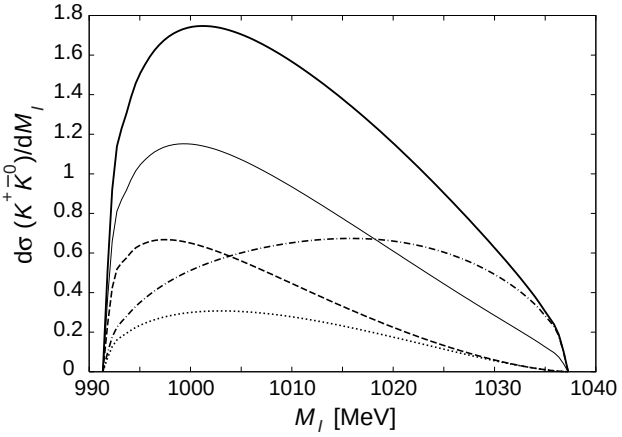

Fig. 4. $\mathrm{d}\sigma(K^+\bar{K}^0)/\mathrm{d}M_I$ for the whole range of available M_I in the reaction $pp \to dK^+\bar{K}^0$ with $\sqrt{s} = 2912.88$ MeV. The thick (thin) solid line is the full result with $a_{\bar{K}N} = -1.84\,(-1.34)$. The dashed line corresponds to including only meson-meson FSI, the dash-dotted one includes only $\bar{K}^0 d$ FSI and the dotted line includes no FSI with a $\mathbf{p}_d^2$ factor for the modulus squared of the amplitude.

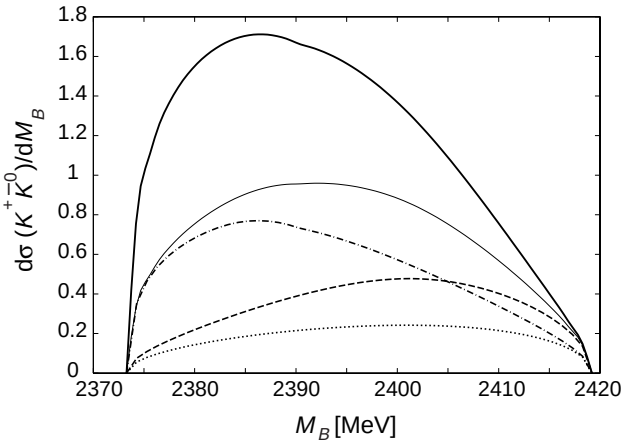

Fig. 5. $\mathrm{d}\sigma(K^+\bar{K}^0)/\mathrm{d}M_B$ for the whole range of available M_B in the reaction $pp \to dK^+\bar{K}^0$ with $\sqrt{s} = 2912.88$ MeV. The thick (thin) solid line is the full result with $a_{\bar{K}N} = -1.84\,(-1.34)$. The dashed line corresponds to including only meson-meson FSI, the dash-dotted one includes only $\bar{K}^0 d$ FSI and the dotted line includes no FSI with a $\mathbf{p}_d^2$ factor for the modulus squared of the amplitude.

about $M_I = 997$ MeV. This is an obvious consequence of the presence of the $a_0(980)$ resonance around 980 MeV and the $K^+\bar{K}^0$ distribution feels the tail of that resonance which increases the strength the closer one is to the resonance position, and hence to smaller values of the $K^+\bar{K}^0$ invariant mass. If one switches on only the $\bar{K}^0 d$ FSI (dash-dotted line) the distribution is rather broad and there is an accumulation of strength to higher values of the M_I. Finally, when all the interactions are considered (thick solid line) the peak of the distribution moves back to lower masses around 1 GeV, where the pure phase space peaks as well. The strength is furthermore increased by about a factor five due to the combined effects of both FSI. The effect of the $\bar{K}^0 d$ interaction moving the peak towards the center of the distribution reflects the fact that for these values of M_I the $\bar{K}^0$ and the deuteron are at rest where $\mathrm{G}_d t_{\bar{K}d}$ has its maximum. Indeed, in the extremes of the M_I distribution either the kaons go together and the deuteron goes opposite to them, or the deuteron is produced at rest and the two kaons go back to back. In both cases the $\bar{K}^0 d$ invariant mass is relatively far from the $\bar{K}^0 d$ threshold situation. In addition, we also include the full result for $a_{\bar{K}N} = -1.3$ presented by the thin solid line. As it is clear this variation in the value of $a_{\bar{K}N}$ mostly decreases the width of the distribution, while the peak position is just slightly decreased by less than 2 MeV. Had we further reduced the value of $a_{\bar{K}N}$, instead of increasing it, the changes would have opposite sense.

Similar changes in strength and shape can be seen in fig. 5 for the $\mathrm{d}\sigma_{K^+\bar{K}^0}/\mathrm{d}M_B$ invariant-mass distribution where the notation for the curves is the same as for fig. 4. It is remarkable that the strong $\bar{K}^0 d$ interaction at threshold pushes the mass distribution towards lower $\bar{K}d$ invariant masses as a reflection of the presence of the $\Lambda(1405)$ resonance in the $\bar{K}^0 n$ system, much as in the case of the $K^+\bar{K}^0$ distribution where the presence of the $a_0(980)$ resonance pushed the distribution towards low $K^+\bar{K}^0$ invariant masses. Here the effects of decreasing the modulus of $a_{\bar{K}N}$ are opposite to those in the $K^+\bar{K}^0$ mass distribution pushing the distribution to higher invariant masses.

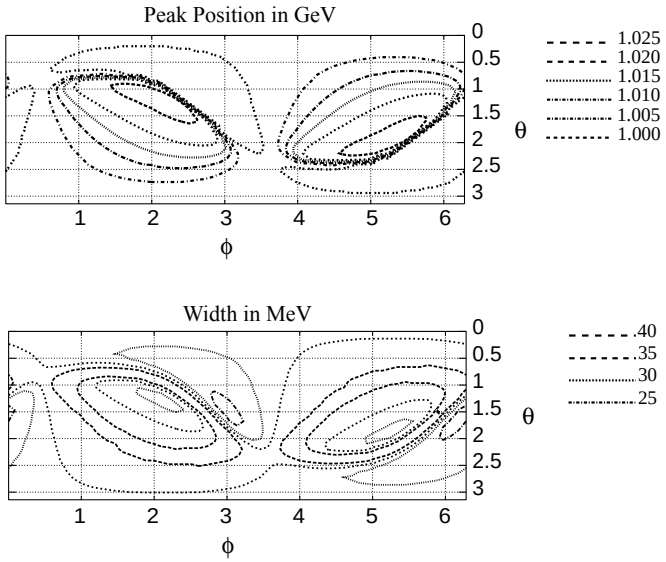

Fig. 6. The upper panel shows the peak position of $\mathrm{d}\sigma(K^+\bar{K}^0)/\mathrm{d}M_I$ and the lower one the width of the same distribution for $a_{\bar{K}N} = -1.84$ as functions of θ and ϕ (in radians).

In fig. 6 we show as a function of θ and ϕ the peak position of the $\mathrm{d}\sigma_{K^+\bar{K}^0}/\mathrm{d}M_I$ distribution and its width. The width is defined to be the difference between the values of M_I for which the number of events is half of the maximum value. The same is shown in fig. 7 for a different value of the subtraction constant $a_{\bar{K}N}$, *i.e.* $a_{\bar{K}N} = -1.3$. The advantage of these figures is that one can approximately describe the shape of the distribution as a function of θ and ϕ.

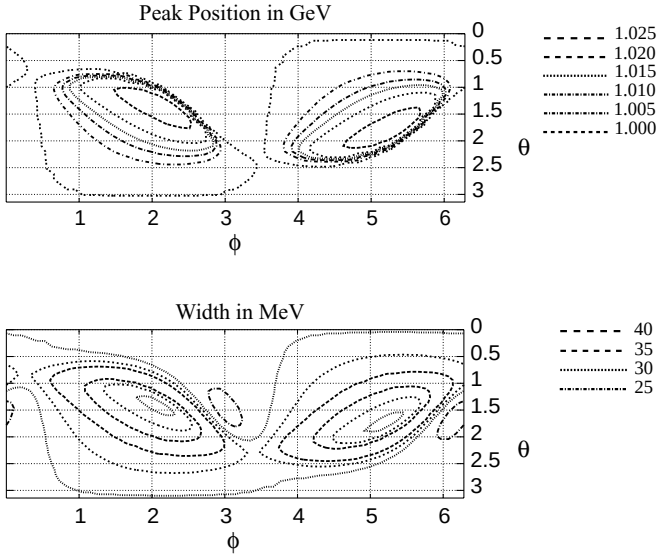

Fig. 7. The upper panel shows the peak position of $\mathrm{d}\sigma(K^+\bar{K}^0)/\mathrm{d}M_I$ and the lower one the width of the same distribution for $a_{\bar{K}N} = -1.3$ as functions of θ and ϕ (in radians).

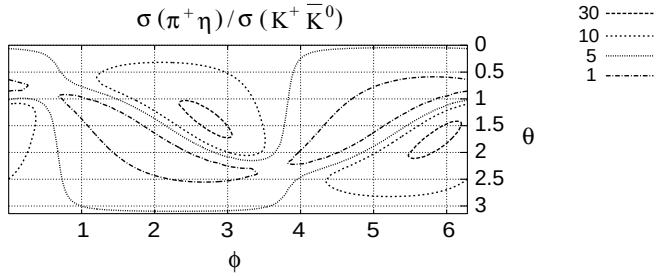

Fig. 8. $\sigma(\pi^+\eta)/\sigma(K^+\bar{K}^0)$ as a function of θ and ϕ (in radians). $M_I(\pi^+\eta) > 950$ MeV when calculating $\sigma(\pi^+\eta)$.

Next, we investigate the role of the θ and ϕ parameters in the total production of $\pi^+\eta$ and $K^+\bar{K}^0$. The $\pi^+\eta$ production is mostly done around the $a_0(980)$ resonance region. In fig. 8 we show the ratio between the integrated $\pi^+\eta$ production cross-section between $M_I = 950$ MeV and the end of its phase space and the $K^+\bar{K}^0$ production cross-section in all its available phase space. We can see in the figure that for most of the values of θ and ϕ the $\pi^+\eta$ production rate is substantially larger than that of $K^+\bar{K}^0$. It is interesting to point out that even in the case when there is no primary $\pi^+\eta$ production so that $f^S_{\pi\eta} = 0$ ($\theta = 0$ and any ϕ or $\phi = \pi/2$, $3\pi/2$ and any θ), the final-state interactions starting from primary $K^+\bar{K}^0$ production can lead to a $\pi^+\eta$ cross-section an order of magnitude bigger than that of the $K^+\bar{K}^0$. One also finds interesting interference effects for some values of θ and ϕ that can reinforce the $\pi^+\eta$ production as compared to the $K^+\bar{K}^0$ as well as other situations when the $K^+\bar{K}^0$ is produced more copiously than the $\pi^+\eta$ channel. The former occurs for values of ϕ around π and 2π and of θ around $\pi/2$ so that $f^S_{K\bar{K}} \simeq 0$ and $f^P_{K\bar{K}} \simeq 0$ with $\sigma(\pi^+\eta) > 30\,\sigma(K^+\bar{K}^0)$, while the latter tends to happen for a wide range of parameters leading to $K^+\bar{K}^0$ invariant-mass distributions peaked at values of M_I higher than 1010 MeV. This spectacular dependence of the ratio of $\pi^+\eta$ to $K^+\bar{K}^0$ production on the values of primary production weights θ and ϕ should obviously serve as a stimulation for the experimental measurement of the $\pi^+\eta$ production cross-section.

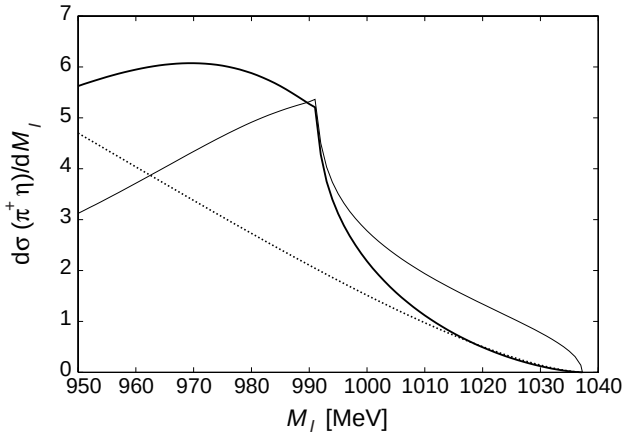

Fig. 9. $\mathrm{d}\sigma(\pi^+\eta)/\mathrm{d}M_I$. Solid line: full result; the dotted line does not include FSI, with a factor $\mathbf{p}_d^2$ from the modulus squared of the amplitude. The thin solid line corresponds to the full result but divided by $\mathbf{p}_d^2$ times 250^2 MeV^2 (to normalize the curve to the full result at the $\bar{K}K$ threshold).

It is interesting to see also the shape of the $\pi^+\eta$ invariant-mass distribution, which is independent of $a_{\bar{K}N}$. We show in fig. 9 by the thick solid line that the normalized $\mathrm{d}\sigma_{\pi^+\eta}/\mathrm{d}M_I$ event distribution for $f^S_{\pi\eta} = 0$ and $f^P_{K\bar{K}}$ = arbitrary ($|f^P_{K\bar{K}}| \leq 1$, see eq. (30)) has no clear signal of the $a_0(980)$ resonance around the values of $M_I = 980$ MeV. This seems somewhat surprising since the coupled-channel approach definitely generates the resonance and we have already observed the effects of its tail in the $K^+\bar{K}^0$ invariant-mass distribution. The lack of resonance structure is due to the P-wave character of the reaction and the appearance of the $|\mathbf{p}_d|^2$ factor in $|F_{\pi^+\eta}|^2$. This factor grows as the invariant mass decreases and distorts the $a_0(980)$ shape. In fact it is interesting to observe that if we divide $\mathrm{d}\sigma_{\pi^+\eta}/\mathrm{d}M_I$ by $|\mathbf{p}_d|^2$, which is also shown in the figure by the thin solid line, the resonance shape appears with a width of around 40 MeV and with the peak at 990 MeV. Noticing this fact is also important from the experimental point of view in order to extract properties of the $a_0(980)$ resonance in this reaction.

We can see that the distributions are rather dependent on the values of the θ and ϕ. This fact could be used to extract the optimal parameters from the data on $K^+\bar{K}^0$ distributions, assuming that a good fit is possible. Should this be the case, the theory would then predict absolute rates and mass distribution for the $\pi^+\eta$ production or other experimental yields, which would be a real prediction of the approach in spite of having started from two unknown parameters.

5 Conclusions

In this paper we have performed a phenomenological study of the $pp \to dK^+\bar{K}^0$ and $pp \to d\pi^+\eta$ reactions close to threshold presently studied by the ANKE collaboration at COSY. We have emphasized the relevance of the final-state interactions which is quite important in the present case due to the proximity of the $K^+\bar{K}^0$ system to the $a_0(980)$ resonance and the $\bar{K}^0 n$ system to the $\Lambda(1405)$ resonance. We found that the consideration of these interactions has important consequences both in the shape and strength of the invariant-mass distributions. We also studied the interaction of the two final states $K^+\bar{K}^0$ and $\pi^+\eta$ by means of a coupled-channel chiral unitary approach which generates both the $a_0(980)$ and $\Lambda(1405)$ resonances. Given the freedom in the primary production amplitudes we parameterize them in terms of three types of structures involving $\ell = 1,\ L = 0$ and $\ell = 0,\ L = 1$ for the $K^+\bar{K}^0$ channel and the only allowed $\ell = 1, L = 1$ for $\pi^+\eta$ production. This left us with two independent parameters (up to a global normalization of one cross-section) together with a subtraction constant with an expected uncertainty of about 25%. The sensitivity of the shapes of the $K^+\bar{K}^0$ and $\bar{K}^0 d$ invariant-mass distributions to those parameters was investigated anticipating that the measurements of these quantities could serve to fix them. This would allow us to make absolute predictions for $\pi^+\eta$ production due to the dynamics of coupled channels generated in the chiral unitary scheme followed here. Other quantities which might be measured could also be predicted in that case. Furthermore, we observed that the $\pi^+\eta$ production was dominated by the $a_0(980)$ resonance and that a clear signal for the relevance of the $\bar{K}^0 d$ FSI would be the observation of a peak towards low $\bar{K}^0 d$ invariant masses in the $\mathrm{d}\sigma_{K^+\bar{K}^0}/\mathrm{d}M_B$ differential cross-section. On other hand, we have also pointed out that the $a_0(980)$ would not be clearly visible in the data for $\mathrm{d}\sigma_{\pi^+\eta}/\mathrm{d}M_I$ because of the $|\mathbf{p}_d|^2$ factor due to the P-wave character of the reaction which distorts the shape of the resonance. Yet we found that the shape of the resonance was regained by dividing $\mathrm{d}\sigma_{\pi^+\eta}/\mathrm{d}M_I$ by $|\mathbf{p}_d|^2$.

Finally, we have also provided general expressions to take into account the FSI derived in this paper for any other more specific model of the primary production mechanism.

The study done here clearly shows how the measurements performed or planned with those reactions provide basic information on the strong interaction underlying the meson-meson and meson-baryon dynamics and should produce complementary and valuable information to the one obtained from other processes.

One of us (E.O.) would like to acknowledge the hospitality of the Institut für Kernphysik des Forschungszentrum Jülich where this work was carried out. We appreciate useful discussions with K. Kilian and H. Ströher, V. Koptev, M. Büscher, A. Sibirtsev and other members of the ANKE collaboration. This paper is partially supported by the DGICYT contract number BFM 2000-1326, the EU TMR network Eurodaphne, contract no. ERBFMRX-CT98-0169 and the Deutsche Forschungsgemeinschaft.

Appendix A. General structure of the process pp → dPQ

Let us denote by ℓ the relative orbital angular momentum of the deuteron and the CM motion of the two pseudoscalar system PQ and by L the orbital angular momentum of the latter in their own CM frame. As discussed in sect. 2 close to the $dK^+\bar{K}^0$ threshold the leading contribution stems from $\ell = 1,\ L = 0$ and $\ell = 0,\ L = 1$. We denote by ℓ_0 the orbital angular momentum of the two protons in the initial state and, as also discussed above, the only possibilities are $\ell_0 = 1,\ 3$. Finally, the symbol S^d refers to the total spin of the deuteron, $S^d = 1$, with its third component indicated by S_3^d. Analogously S refers to the total spin of the pp system, which is also fixed to be 1, and S_3 indicates its third component.

Keeping only the components relevant for our reaction, we can consider the following angular momentum decomposition of the final dPQ state as:

$$|d(S_3^d,\mathbf{p}_d)P(\mathbf{k}_1)Q(\mathbf{k}_2)\rangle \propto \sum_{m,J} C(S_3^d\ m|1\ 1\ J)\Big(\mathrm{Y}_{1m}(\hat{p}_d)^* \times |J, S_3+m; \ell=1, L=0\rangle + \mathrm{Y}_{1m}(\hat{k})^*|J, S_3+m; \ell=0, L=1\rangle\Big) + \dots, \tag{A.1}$$

where $\mathbf{k}$ is the PQ-CM three momentum of the pseudoscalar P, the symbol $C(m_1\ m_2|j_1\ j_2\ J)$ is the Clebsch-Gordan coefficient for the composition of two angular momenta j_1 and j_2 to give the total one J and the ellipses simply denote other terms of no interest here. It is worth noting once again that for the $\pi^+\eta$ system only the $\ell = 1,\ L = 0$ component is relevant due to the absence of resonant interactions of this system with the deuteron. Performing an analogous decomposition for the initial pp state we can write for the transition matrix element:

$$\langle d(S_3^d,\mathbf{p}_d)P(\mathbf{k}_1)Q(\mathbf{k}_2)|T|p(\mathbf{p}_1)p(\mathbf{p}_2),S_3\rangle = \sum_{J,\ell_0} C(S_3^d\ S_3-S_3^d|1\ 1\ J)\ C(S_3\ 0|1\ \ell_0\ J)\ \mathrm{Y}_{1\,0}(\hat{p}_1)^* \times \Big(\mathrm{Y}_{1\,S_3-S_3^d}(\hat{p}_d)T_{10\ell_0}^{J\,PQ} + \mathrm{Y}_{1\,S_3-S_3^d}(\hat{k})T_{01\ell_0}^{J\,PQ}\Big)\ , \tag{A.2}$$

where $\mathbf{p}_1 = (0, 0, |\mathbf{p}_1|)$ and because of the small velocities involved at around the $dK^+\bar{K}^0$ threshold we can also write $\mathrm{Y}_{1m}(\hat{p}_\ominus)$ instead of $\mathrm{Y}_{1m}(\hat{k})$ with $\mathbf{p}_\ominus$ defined in sec. 3. Note as well that we take the invariant-matrix elements $T_{01\ell_0}^{J\,\pi\eta} = 0$, due to the absence of any resonant S-wave interaction between the $\pi^+\eta$ system and the deuteron. In order to take care of the final-state interactions due to both the meson-meson and $\bar{K}d$ S-wave interactions one can proceed in a completely analogous way to that of sect. 3. First we define the related quantities $T_{10\ell_0}^{J\,PQ} = |\mathbf{p}_d|A_{10\ell_0}^{J\,PQ}$ and

$T^{J\,PQ}_{01\ell_0} = |\mathbf{p}_\ominus| A^{J\,PQ}_{01\ell_0}$ and second the $A^{J\,PQ}_{\ell L\ell_0}$ can be taken, if desired, as constants. In this way one has:

$$
\begin{aligned}
F_{\pi^+\eta} &= |\mathbf{p}_d| \mathrm{Y}_{1\,S_3-S_3^d}(\hat{p}_d) \sum_{J,\ell_0} \mathrm{Y}_{\ell_0\,0}(\hat{p}_1)^* \\
&\times C(S_3^d\ S_3 - S_3^d | 1\ 1\ J) C(S_3\ 0 | 1\ \ell_0\ J) \\
&\times \left([\mathcal{D}^{-1}(M_I^2)]_{11} A^{J\,\pi\eta}_{10\ell_0} + [\mathcal{D}^{-1}(M_I^2)]_{12} A^{J\,K\bar{K}}_{10\ell_0} \right) , \\
F_{K^+\bar{K}^0} &= |\mathbf{p}_d| \mathrm{Y}_{1\,S_3-S_3^d}(\hat{p}_d) \sum_{J,\ell_0} \mathrm{Y}_{\ell_0\,0}(\hat{p}_1)^* \\
&\times C(S_3^d\ S_3 - S_3^d | 1\ 1\ J) C(S_3\ 0 | 1\ \ell_0\ J) \\
&\times \left([\mathcal{D}^{-1}(M_I^2)]_{21} A^{J\,\pi\eta}_{10\ell_0} + [\mathcal{D}^{-1}(M_I^2)]_{22} A^{J\,K\bar{K}}_{10\ell_0} + A^{J\,K\bar{K}}_{01\ell_0} \right) \\
&+ |\mathbf{p}_{K^+}| \mathrm{Y}_{1\,S_3-S_3^d}(\hat{p}_{K^+}) \sum_{J,\ell_0} \mathrm{Y}_{\ell_0\,0}(\hat{p}_1)^* \\
&\times C(S_3^d\ S_3 - S_3^d | 1\ 1\ J) C(S_3\ 0 | 1\ \ell_0\ J) \\
&\times \left[\frac{-M_d}{M_d + m_K} \mathrm{G}_d(\widetilde{M}_B^2)\, t_{\bar{K}d}(\widetilde{M}_B) A^{J\,K\bar{K}}_{10\ell_0} \right. \\
&+ \left. \left(2 + \frac{M_d + 2m_K}{M_d + m_K} \mathrm{G}_d(\widetilde{M}_B^2)\, t_{\bar{K}d}(\widetilde{M}_B) \right) A^{J\,K\bar{K}}_{01\ell_0} \right] . \qquad \text{(A.3)}
\end{aligned}
$$

Once a model for the primary production mechanism of the PQ systems is developed, the functions $T^{J\,PQ}_{\ell L\ell_0}$ can be determined and from them the FSI can be taken into account by eq. (A.3). We can do this exercise for our previous model by comparing eq. (A.2) of the present appendix with eq. (9), times the appropriate couplings constant f^S_{PQ} or $f^P_{K\bar{K}}$. Taking $\ell_0 = 1$, since our model only involves one power of $\mathbf{p}_1$, we then have:

$$
\begin{aligned}
&T^{0\,K\bar{K}}_{1\,0\,1} = -4\sqrt{3\pi} f^S_{K\bar{K}} |\mathbf{p}_1||\mathbf{p}_d| , \\
&T^{0\,K\bar{K}}_{0\,1\,1} = -4\sqrt{3\pi} f^P_{K\bar{K}} |\mathbf{p}_1||\mathbf{p}_\ominus| , \\
&T^{1\,K\bar{K}}_{1\,0\,1} = \frac{8\sqrt{\pi}}{\sqrt{3}} f^S_{K\bar{K}} |\mathbf{p}_1||\mathbf{p}_d| , \quad T^{1\,K\bar{K}}_{0\,1\,1} = \frac{8\sqrt{\pi}}{\sqrt{3}} f^P_{K\bar{K}} |\mathbf{p}_1||\mathbf{p}_\ominus|, \\
&T^{2\,K\bar{K}}_{101} = 0 , \qquad\qquad T^{2\,K\bar{K}}_{010} = 0 , \\
&T^{0\,\pi\eta}_{1\,0\,1} = -4\sqrt{3\pi} f^S_{\pi\eta} |\mathbf{p}_1||\mathbf{p}_d| , \quad T^{1\,\pi\eta}_{1\,0\,1} = \frac{8\sqrt{\pi}}{\sqrt{3}} f^S_{\pi\eta} |\mathbf{p}_1||\mathbf{p}_d|, \\
&T^{2\,\pi\eta}_{101} = 0 . \qquad\qquad \text{(A.4)}
\end{aligned}
$$

References

1. S. Barsov et al., Nucl. Instrum. Methods A **462**, 364 (2001); M. Büscher et al., COSY proposal #55, `http://www.fz-juelich.de/ikp/anke`.
2. V.Yu. Grishina, L.A. Kondratyuk, E.L. Bratkovskaya, M. Büscher, W. Cassing, Eur. Phys. J. A **9**, 277 (2000).
3. E.L. Bratkovskaya, V.Yu. Grishina, L.A. Kondratyuk, M. Büscher, W. Cassing, nucl-th/0107071.
4. M. Büscher, V. Kleber (Editors), *Workshop on* $a_0(980)$ *physics with ANKE*, Berichte des Forschungszentrum Jülich, 2000, ISSN 0944-2952.
5. N.A. Tornqvist, Phys. Rev. Lett. **49**, 624 (1982); N.A. Tornqvist, M. Roos, Phys. Rev. Lett. **76**, 1575 (1996).
6. R. Jaffe, Phys. Rev. D **15**, 267; 281 (1977).
7. N.N. Achasov, N.N. Achasov, S.A. Devyanin, G.N. Shestakov, Sov. J. Nucl. Phys. **32**, 566 (1980); (Yad. Fiz. **32**, 1098 (1980)).
8. E. van Beveren, T.A. Rijken, K. Metzger, C. Dullemond, G. Rupp, J.E. Ribeiro, Z. Phys. C **30**, 615 (1986); E. van Beveren, G. Rupp, Eur. Phys. J. C **22**, 493 (2001), hep-ex/0106077.
9. D. Black, A.H. Fariborz, S. Moussa, S. Nasri, J. Schechter, Phys. Rev. D **64**, 014031 (2001); D. Black, A.H. Fariborz, J. Schechter, hep-ph/0008246.
10. J. Weinstein, N. Isgur, Phys. Rev. Lett. **48**, 659 (1982); Phys. Rev. D **27**, 588 (1983); **41**, 2236 (1990).
11. C. Amsler, F.E. Close, Phys. Rev. D **53**, 295 (1996); C. Amsler, in *Proceedings of Hadron Spectroscopy*, edited by T. Bressani, A. Feliciello, A. Filippi, Frascati Physics Series, Vol. **15** (INFN, Frascati, 1999) p. 609.
12. D. Morgan, Phys. Lett. B **51**, 71 (1974); K.L. Au, D. Morgan, M.R. Pennington, Phys. Rev. D **35**, 1633 (1987); D. Morgan, M.R. Pennington, Z. Phys. C **37**, 431 (1988); Phys. Lett. B **258**, 444 (1991); **269**, 477 (1991) (E); Phys. Rev. D **48**, 1185; 5422 (1993); M.R. Pennington, S.N. Cherry, Nucl. Phys. A **688**, 823 (2001).
13. U.-G. Meißner, Comments Nucl. Part. Phys. **20**, 119 (1991).
14. V.E. Markushin, Eur. Phys. J. A **8**, 389 (2000); V.E. Markushin, Zi-guang Xiao, H.Q. Zheng, hep-ph/0011260; Zhi-guang Xiao, H.Q. Zheng, hep-ph/0103042.
15. B. Moussallam, Eur. Phys. J. C **14**, 111 (2000); S. Descotes, L. Girlanda, J. Stern, JHEP 0001(2000)041; S. Descotes, JHEP 0103(2001)002; L. Girlanda, J. Stern, P. Talavera, Phys. Rev. Lett. **86**, 5858 (2001).
16. A. Bramon, R. Escribano, J.L. Lucio, M. Napsuciale, G. Pancheri, Phys. Lett. B **494**, 221 (2000); A. Bramon, R. Escribano, J.L. Lucio Martinez, M. Napsuciale, Phys. Lett. B **517**, 345 (2001), hep-ph/0105179.
17. E. Klempt, B.C. Metsch, C.R. Münz, H.R. Petry, Phys. Lett. B **361**, 160 (1995).
18. G. Janssen, B.C. Pearce, K. Holinde, J. Speth, Phys. Rev. D **52**, 2690 (1995).
19. A. Dobado, M.J. Herrero, T.N. Truong, Phys. Lett. B **235**, 134 (1990); A. Dobado, J.R. Peláez, Phys. Rev. D **56**, 3057 (1997); T. Hannah, Phys. Rev. D **55**, 5613 (1997); J.A. Oller, E. Oset, J.R. Peláez, Phys. Rev. Lett. **80**, 3452 (1998); Phys. Rev. D **59**, 074001 (1999); **60**, 099906 (1999)(E); F. Guerrrero, J.A. Oller, Nucl. Phys. B **537**, 459 (1999); T. Hannah, Phys. Rev. D **60**, 017502 (1999); A. Gómez Nicola, J.R. Peláez, hep-ph/0109056.
20. J. Nieves, E. Ruiz Arriola, Phys. Lett. B **455**, 30 (1999); Nucl. Phys. A **679**, 57 (2000).
21. V. Elias, A.H. Fariborz, Fang Shi, T.G. Steele, Nucl. Phys. A **633**, 279 (1998); T.G. Steele, Fang Shi, V. Elias, in *Proceedings of Hadron Spectroscopy*, edited by T. Bressani, A. Feliciello, A. Filippi, Frascati Physics Series, Vol. **15** (INFN, Frascati, 1999) p. 217; hep-ph/9905303; T.G. Steele, D. Harnett, hep-ph/0108232.
22. S. Narison, Nucl. Phys. A **675**, 54 (2000)c.

23. J.A. Oller, E. Oset, Nucl. Phys. A **620**, 438 (1997); **652**, 407 (1999) (E).
24. J.A. Oller, E. Oset, Phys. Rev. D **60**, 074023 (1999).
25. J.A. Oller, E. Oset, Nucl. Phys. A **629**, 739 (1998).
26. J.A. Oller, Phys. Lett. B **426**, 7 (1999).
27. E. Marco, S. Hirenzaki, E. Oset, H. Toki, Phys. Lett. B **470**, 20 (1999).
28. U.-G. Meißner, J.A. Oller, Nucl. Phys. A **679**, 671 (2001).
29. N. Kaiser, P.B. Siegel, W. Weise, Nucl. Phys. A **594**, 325 (1995); N. Kaiser, T. Waas, W. Weise, Nucl. Phys. A **612**, 297 (1997).
30. E. Oset, A. Ramos, Nucl. Phys. A **635**, 99 (1998).
31. J.A. Oller, U.-G. Meißner, Phys. Lett. B **500**, 263 (2001).
32. R.H. Dalitz, T.C. Wong, G. Rajasekaran, Phys. Rev. **153**, 1617 (1967).
33. E. Oset, A. Ramos, C. Bennhold, to be published in Phys. Lett. B., nucl-th/0109006.
34. Amsterdam-CERN-Nijmegen-Oxford Collaboration, Phys. Lett. B **63**, 220 (1976).
35. T.A. Armstrong et al, Z. Phys. C **52**, 389 (1991).
36. D.E. Groom et al., Eur. Phys. J. C **15**, 1 (2000).
37. A. Gokalp, O. Yilmaz, Phys. Rev. D **64**, 053017 (2001).
38. J. Gasser, H. Leutwyler, Nucl. Phys. B **250**, 465 (1985).
39. U.-G. Meißner, Rep. Prog. Phys. **56**, 903 (1993).
40. A. Pich, Rep. Prog. Phys. **58**, 563 (1995).
41. U.-G. Meißner, E. Oset, A. Pich, Phys. Lett. B **353**, 161 (1995).
42. V. Chernyshev, P.V. Fedorets, A.E. Kudryavtsev, V.E. Tarasov, ANKE preprint.
43. V. Bernard, N. Kaiser, U.-G. Meißner, Phys. Rev. D **44**, 3698 (1991).
44. G. Ecker, J. Gasser, A. Pich, E. de Rafael, Nucl. Phys. B **321**, 311 (1989).
45. N. Kaiser, Eur. Phys. J. A **3**, 307 (1998).
46. J.A. Oller, E. Oset, A. Ramos, Prog. Part. Nucl. Phys. **45**, 157 (2000).
47. J.A. Oller, invited talk at *Workshop on Possible Existence of the sigma meson and its Implications to Hadron Physics (sigma-meson 2000) YITP, Kyoto, Japan, 12-14 June 2000*, hep-ph/0007349.
48. J.A. Oller, E. Oset, J. Palomar, Phys. Rev. D **63**, 114009 (2001).
49. G. Toker, A. Gal, J.M. Eisenberg, Nucl. Phys. A **362**, 405 (1982).
50. M. Torres, R.H. Dalitz, A. Deloff, Phys. Lett. B **174**, 213 (1986).
51. A. Bahaoui, C. Fayard, G.H. Lamot, T. Mizutani, Nucl. Phys. A **508**, 335 (1990).
52. R.C. Barrett, A. Deloff, Phys. Rev. C **60**, 025201 (1999).
53. A. Deloff, Phys. Rev. C **61**, 024004 (2000).
54. S.S. Kamalov, E. Oset, A. Ramos, Nucl. Phys. A **690**, 494 (2001).